The Measurement of Monopulse Tracking Nulls in a Planar Near-field Antenna Range

Daniël Janse van Rensburg & Pieter Betjes
Nearfield Systems Inc
19730 Magellan Drive
Torrance, CA, 90503, USA
drensburg@nearfield.com & pbetjes@nearfield.com

***Abstract*—Monopulse antennas typically have a sum and two difference channels allowing for the accurate tracking of radar targets. Measuring the radiation patterns of these three channels often include establishing the electrical boresight of the antenna. Planar near-field test systems allow for the accurate determination of difference pattern nulls and locations. In this paper we present an iterative process requiring the use of all three channels to achieve an accurate null depth and location result. The impact of near-field truncation on the boresight pointing angle is also addressed and achievable accuracy numbers are presented.**

Keywords – Monopulse antenna, Tracking, Planar near-field, Boresight error.

I. Introduction

Monopulse radar systems rely on monopulse antennas which typically are three port devices. These ports are commonly designated as sum, difference elevation and difference azimuth [1]. The sum port is typically used during the transmission phase of the radar for target illumination and the two difference ports of the antenna during the receive phase of the radar for target detection and tracking. Monopulse antennas usually consist of four independently controlled quadrants where the sum pattern is generated by in-phase excitation of these quadrants, the difference elevation pattern is generated by out of phase excitation of the top and bottom quadrant pairs and the difference azimuth pattern is generated by out of phase excitation of the left and right quadrant pairs. The signal manipulation to obtain these three distinct signals is usually performed in hardware using a monopulse comparator. This component is integrated with the antenna feed structure, although measuring the four quadrants individually and performing the complex mathematics to derive the three signals is also feasible with modern test equipment.

When testing these types of antennas, the specific radiation pattern properties related to monopulse radar operation that are relevant, include: Difference pattern null depth, null slope and null location. Traditionally these parameters are measured in a far-field or a compact antenna test range. In this paper we describe how this can be done using a planar near-field [2, 3] facility. In Section II a description of the alignment procedure unique to this type of test process is given. In Section III we present typical radiation pattern data for a monopulse antenna and show how a planar near-field (PNF) test allows one to form a two dimensional image of the pattern behavior for each individual antenna port. These images then have to be analyzed collectively to determine the antenna electrical pointing angles and effective null depths. The null searching process is described in Section IV and in Section V we show how the null locations are affected by near-field truncation and how this problem can be addressed.

II. AUT Alignment in Planar Near-field Ranges

Matching electrical beam pointing to a mechanical reference (boresight determination) is crucial for tracking antennas. An angular difference observed is commonly referred to as electrical pointing or boresight error. Any uncertainty in these error values are highly undesirable and are typically less than 1 mrad (0.057°). These tight tolerances place very stringent requirements on rotary positioners when using far-field or compact range test methods. When using a PNF test technique, there is no motion of the antenna under test (AUT) and the PNF scan plane (ideally flat) becomes the alignment reference plane [4, 5]. In Fig. 1 below a typical test setup is shown with the PNF test probe on the left and the AUT (a slotted waveguide array) on the right.

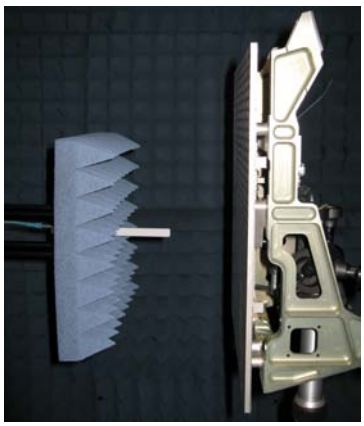

Figure 1: A typical PNF test setup with the probe on the left and the AUT on the right.

Alignment of the AUT parallel to the scan plane is the objective in this instance and this is achieved as depicted in Fig. 2. By measuring the differential distance between the probe tip and the face of the AUT at two extremities and considering the distance between the two measurements an angular offset can be calculated. For the case shown here an AUT width of 240 mm is assumed and a differential distance of 0.06 mm (achievable using a dial indicator) leading to an angular offset of 0.244 mrad (0.014°).

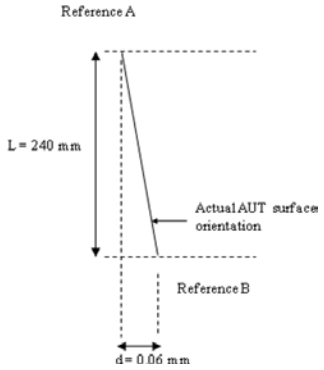

Figure 2: By measuring the differential distance between the probe tip and the face of the AUT at two extremities and considering the distance between the two measurements an angular offset can be calculated.

This angular offset can now be removed by adjusting the AUT to be parallel to the PNF scan plane. Repeating this process for both the horizontal and vertical planes, allows one to align the AUT in two dimensions. It is important to realize that angular tilt alone and not lateral displacement between the probe tip and AUT, affects measured electrical pointing. It should also be noted that when this alignment is done the operator has to ensure that the surface of measurement on the AUT should be a precision alignment surface. Often times this is on the back of the AUT, in which case special alignment fixturing is required to allow one to measure the probe tip to AUT alignment surface distance.

III. Typical Monopulse Radiation Patterns

Fig. 3 – 5 below show typical far-field principal polarization radiation patterns for a monopulse antenna. The three images show the sum, difference elevation and difference azimuth patterns respectively, all in an azimuth over elevation coordinate system over a span of 40 degrees. (In this instance this coordinate system has been selected to emulate the AUT operational positioner.) The on-axis nulls for both difference patterns can be identified and it is important to note that these nulls are well defined in only a single dimension. Enlarging the detail for both null locations (shown in Fig. 6 & 7), it can be seen that the lowest amplitude regions (red contours show < -40 dB) are not located at the (0,0) location and multiple regions of this low amplitude can be identified. The ramification of this phenomenon is that a simple null searching routine will not locate the true monopulse null of the antenna and an alternative scheme is needed.

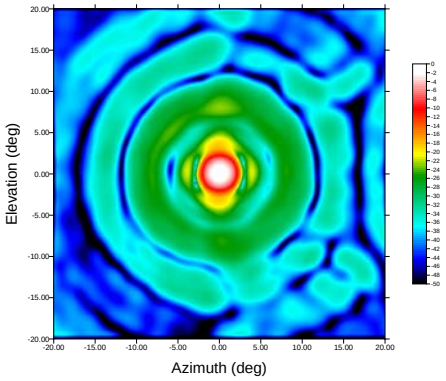

Figure 3. Typical monopulse antenna sum beam radiation pattern shown over a 40° span in an azimuth/elevation coordinate system.

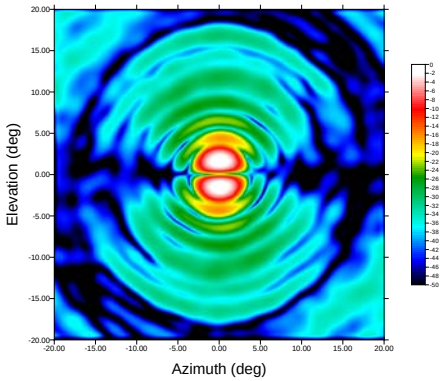

Figure 4. Typical monopulse antenna elevation difference radiation pattern shown over a 40° span in an azimuth/elevation coordinate system.

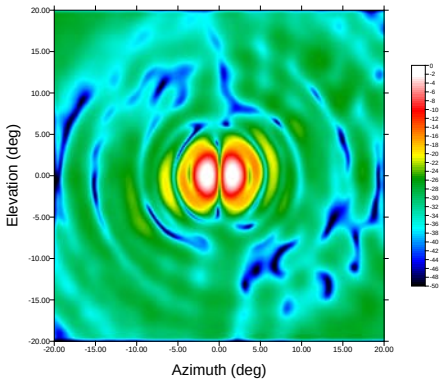

Figure 5. Typical monopulse antenna azimuth difference radiation pattern shown over a 40° span in an azimuth/elevation coordinate system.

IV. Null Searching Routine

In order to uniquely locate the monopulse antenna nulls and resulting electrical pointing error the three signals available at the antenna ports cannot be considered in isolation. Since these signals are combined by the radar system a process similar to that employed by the radar is used for null pointing determination. Fig. 8 shows an overlay of the azimuth and elevation pattern null contours (enlarged over an angular span of only 0.2°), showing the orthogonality of the nulls and differening null depth regions. These contours define our region of null search operation. The process involves

determining the sum beam peak as an angular starting location. This process is by no means highly accurate, but simply serves to establish an initial angular position for subsequent null searching iterations. Starting at this location, say (0,0) and then turning to the elevation difference pattern first, a search for the minimum amplitude along the azimuth = 0 cut will lead to location El_1. Starting from this new location (0, El_1) and then turning to the azimuth difference pattern, a search for the minimum amplitude along the El_1 cut will lead to location Az_1 and the process is repeated. This can be continued until subsequent changes observed are less than the desired specification.

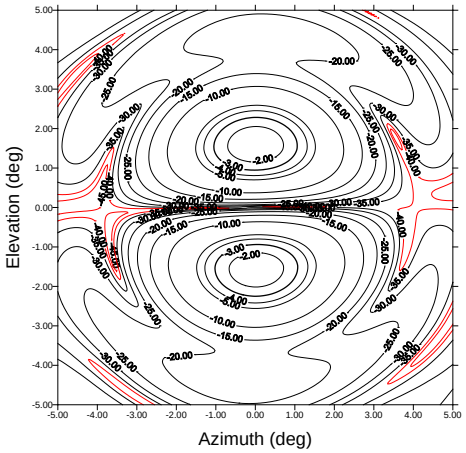

Figure 6. Typical monopulse antenna elevation difference radiation pattern shown over a 10° span in an azimuth/elevation coordinate system with levels < -40 dB shown in red.

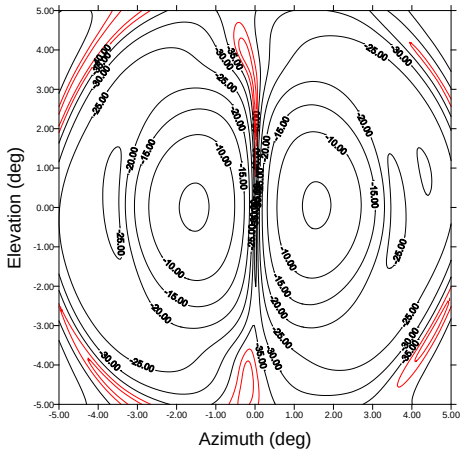

Figure 7. Typical monopulse antenna azimuth difference radiation pattern shown over a 10° span in an azimuth/elevation coordinate system with levels < -40 dB shown in red.

The null determination used here is based on a Fast Fourier Transform (FFT) process and it is therefore advisable to perform the entire search algorithm for a second time using a double density FFT, in order to estimate the influence of the finite resolution of the FFT process. Fig. 8 clearly shows the orthogonal nature of the two nulls in question and the process described leads to a null location within 2 or 3 iterations within the region highlighted by the red ellipse.

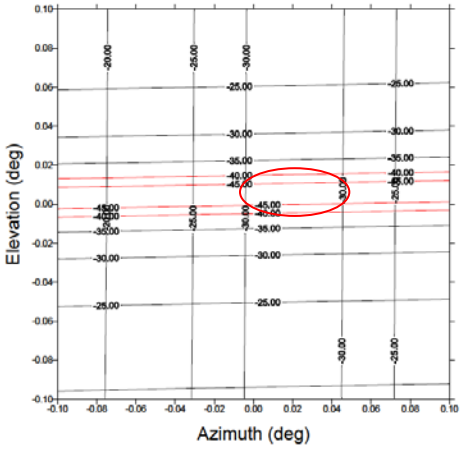

Figure 8: Overlay of the azimuth and elevation pattern null contours, showing the orthogonality of the nulls and differening null depth regions. Final null location within the red elliptical region shown.

V. The Impact Of Near-field Truncation

Truncation of near-field data is a fundamental limitation of the PNF measurement technique [6, 7] and it is important to assess the impact of this on the null location process. Looking at near-field amplitude data for the elevation difference channel it is clear that a full scan plane of 1.48 m x 1.48 m (red curve shown in Fig. 9) leads to truncation at a normalized level of roughly -22 dB. Further truncation of this near-field data to a reduced scan plane of 1 m x 1 m (blue curve shown in Fig. 9) leads to data being truncated at roughly -10 dB. By systematically reducing the scan plane region and extracting azimuth and elevation null locations the data shown in Fig. 10 (green and purple curves respectively) are obtained. It is clear from these curves that the null locations vary significantly as the scan plane size is reduced and truncation effects become more severe.

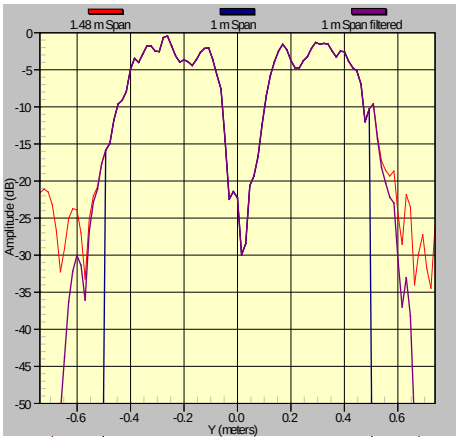

Figure 9: Near-field data shown for full 1.48 m span (red), truncated to 1 m span (blue) and near-field filtered at 1 m (purple).

If one applies a filter function to the near-field amplitude data as depicted in Fig. 9, the impact of the truncation on the null locations can be reduced. This is depicted by the blue and red curves in Fig. 10. The worst case null variation as a result

of near-field truncation without this filter function is roughly 0.2 mrad. With near-field filtering this variation is reduced to about 0.05 mrad. We do not recommend using near-field filtering blindly since this is data altering. However, it is a valuable tool that allows one to assess the impact of truncation and the fundamental conclusion to be drawn here is that monopulse null locations are susceptible to near-field truncation and this should be considered when establishing a PNF test process for these types of antennas.

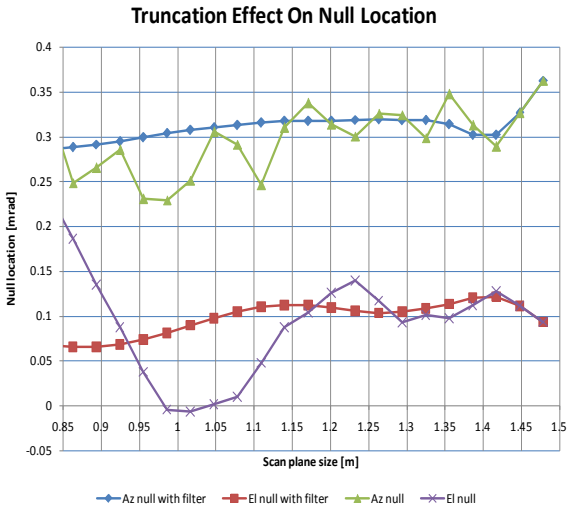

Figure 10: Azimuth and elevation null locations shown as a function of scan plane size, with and without near-field filtering.

VI. Conclusion

We have shown how an antenna can be aligned on a planar near-field range to establish electrical pointing. A technique for the location of the difference pattern nulls of monopulse antennas has also been presented. This process couples the two monopulse difference channels to obtain a unique system level null location. The effect of near-field truncation on these null locations has also been demonstrated. Near-field filtering can be used as a technique for softening the truncation effect. The data presented here shows that PNF antenna testing can be used for sub-milliradian pointing alignment of antennas without requiring any motion of the antenna or mechanical searching for nulls.

References

[1] M. I. Skolnik, Introduction To Radar Systems. McGraw Hill, 1983.

[2] D. M. Kerns, Plane-Wave Scattering-Matrix Theory of Antennas and Antenna-Antenna Interactions, National Bureau of Standards Monograph 162, June 1981.

[3] D. Slater, Near-Field Antenna Measurements, Artech House, 1991.

[4] J. H. Wang, "An examination of the theory and practices of planar near-field measurement", IEEE Trans. Antennas & Propagat., Vol. 36, No. 6, June 1988, pp. 746-753.

[5] A. Yaghjian, "An overview of near-field antenna measurements", IEEE Trans. Antennas & Propagat., Vol. AP-34, No. 1, January 1986, pp. 30-45.

[6] D. J. Janse van Rensburg, "Phased-array simulation for antenna test range design", AMTA 20th Annual Meeting & Symposium, Montreal, Quebec, Canada, Nov. 1998.

[7] D. J. Janse van Rensburg, "On the impact of non-rectangular two dimensional near-field filter functions in planar near-field antenna measurements", AMTA 28th Annual Meeting & Symposium, Austin, TX, USA, Oct. 2006.